Published in "Solid State Sciences 21(): 59–65, 2013"
which should be cited to refer to this work.

The effect of carbon morphology on the $LiCoO_2$ cathode of lithium ion batteries

Nam Hee Kwon*

University of Fribourg, Department of Chemistry, Chemin du Musée 9, CH-1700 Fribourg, Switzerland

Conductive carbon coatings on cathode materials play a critical role in the electrochemical performance of lithium ion batteries due to the increased electronic conductivity and the protective effect of the organic electrolyte on the cathode material. The composite structure of a cathode depends on the physicochemical properties of the carbonaceous materials. We investigated several types of carbonaceous materials in $LiCoO_2$ electrodes. Platelet-shaped graphite provided superior cyclic voltammograms and specific capacities of the $LiCoO_2$ electrodes compared to nanosized spherical carbon black. The platelet-shaped graphite mixed homogeneously with $LiCoO_2$ and coated on $LiCoO_2$ particles in the form of a thin layer via the ball-milling method. However, the nano-carbon black is dense and aggregates during the ball-milling process. The thick coating of nano-carbon black on the $LiCoO_2$ particles, which were observed in backscattered electron images collected during the SEM measurements, made the penetration of the liquid electrolyte through this thick carbon layer difficult.

1. Introduction

The cathodes in lithium ion batteries consist of several materials to create an electronically and ionically conducting composite. These materials include a lithium-containing material (active material such as $LiCoO_2$), a carbon additive and a polymer binder. To maximize the electrochemical performance of a cathode, all of these materials in the electrode, specifically the composite of the carbon and active material, must be well constructed and/or assembled.

Since Goodenough's group reported $LiCoO_2$ material as a lithium-intercalated compound in 1980 [1], $LiCoO_2$ material has been actively studied as a cathode for lithium ion batteries due to its high enough capacity for portable electronic devices. However, only half of the lithium ions ($x = 0.5$) are inserted and extracted electrochemically in the structure of $Li_{1-x}CoO_2$ to produce the electrical energy owing to its structural instability at higher voltage of 4.2 V vs. Li/Li^+ [2,3] and the dissolution of cobalt into the organic electrolyte [4]. Intensive studies have been done to overcome these issues by coating nanosized metal oxides such as Al_2O_3 [5], ZrO_2 [6], or ZnO [7]. In general, $LiCoO_2$ material is mixed with a conducting agent such as carbon in various sources to make a desired cathode for lithium ion batteries [8–13]. Several review articles report about the composite electrode materials containing carbon for lithium ion batteries [14–16].

A carbon coating provides the following positive effects on the performance of cathode materials: (1) it enhances the electronic conductivity of the electrode by functioning as an electron charge transfer media [17,18], (2) it suppresses the dissolution of transition metals from the cathode material by functioning as a physical barrier from the highly acidic electrolyte, and (3) it prevents side reactions between the cathode materials and organic electrolytes by functioning as a protective layer [15,19]. Carbon coatings on the active material can be prepared using various methods such as thermal decomposition, chemical vapor deposition (CVD), mechanical milling etc. The thermal decomposition of organic precursors such as sucrose requires a high temperature (>800 °C) under an inert atmosphere to prevent carbon loss. This process generates a strongly reductive environment, which can easily reduce $LiCoO_2$ to CoO or Co_3O_4 [20]. Therefore, post-treatment methods are more suitable for creating a desired composite of $LiCoO_2$ and carbon (C). Mechanical milling is a simple and inexpensive method compared to the chemical vapor deposition method, which requires high vacuum, longer processes and is more expensive. This milling process can also provide the required intimate contact between $LiCoO_2$ and carbon compared to solution

* Tel.: +41 26 300 87 35; fax: +41 26 300 97 38.
E-mail addresses: namhee.kwon@unifr.ch, nhkwon2011@hotmail.com.

mixing using a surfactant. Therefore, $LiCoO_2$ electrodes prepared by slurry mixing were inhomogeneous due to the large density differences between $LiCoO_2$ (4.9 g cm^{-3}) and carbon (1.8–2.2 g cm^{-3}) and the uncontrolled agglomeration of carbon [13].

The majority of cathode materials are prepared using carbon black, acetylene black, carbon nanotubes (CNT) or graphene to improve the electronic conductivity of the electrode [8–13]. These carbonaceous materials vary in purity, particle size, morphology, and conductivity (ratio of sp^2/sp^3) depending on the manufacturing processes and the carbonaceous sources, as shown by Doeff et al. [21]. In general, carbon black has a spherical shape with a relatively high specific surface area, and it is primarily used for nanosized cathode materials in lithium ion batteries to cover a large surface of active particles, as we have previously demonstrated [22,23]. However, graphite has a platelet-like shape with a lower specific surface area. The physicochemical properties of the employed carbon control the homogeneity between the active cathode material and carbon, the porosity of the composite, and consequently, the total conductivity of the cathode. The combination of the pristine characteristics of carbon and a mixing method to create the composite affect the structure of the cathode composite, which affects the performance of the battery.

Here, we report on the effects of the morphology of the carbon and the structure of the composite on the electrochemical properties of $LiCoO_2$ electrodes.

2. Experimental

Commercial $LiCoO_2$ (Aldrich) powder was ball-milled with various types of carbon for 1 h. Graphite SFG and carbon black C65 were provided by Timcal, Belgium. Graphite SLC was provided by Superior Graphite, Chicago, USA. Ketjenblack 600 carbon black was provided by Akzo Nobel, Germany. After creating a composite of $LiCoO_2$ and carbon via ball-milling, the electrode was prepared on aluminum foil with the composite of carbon-$LiCoO_2$ (C–$LiCoO_2$) and polyvinylidene fluoride (PVDF) in *N*-methyl-2-pyrrolidone (NMP). The weight ratio of the $LiCoO_2$ active material, carbon and binder was 70:20:10. The electrodes were dried under vacuum at 120 °C overnight, and these working electrodes were assembled in Swagelok cells with lithium metal as a counter electrode, ethylene carbonate (EC) and dimethyl carbonate (DMC) mixture (1:1 v/v) with 1 M $LiPF_6$ electrolyte and a separator from Celgard. Potentiostatic and galvanostatic techniques were used to examine the electrochemical properties of the carbon–$LiCoO_2$ composite electrodes.

For the characterization of as-received $LiCoO_2$, as-received carbonaceous materials and the composite materials of C–$LiCoO_2$ prepared by ball milling, the Brunauer–Emmett–Teller (BET) nitrogen adsorption method was used to measure the specific surface areas of the C–$LiCoO_2$ composites obtained after ball-milling and the as-received $LiCoO_2$ and carbon materials. The morphology and the size of the particles were determined using scanning electron microscopy (SEM, Philips XL30) and transmission electron microscopy (TEM).

For the electrochemical property of the composite electrodes, cyclic voltammetry was applied within the voltage window between 2.7 and 4.5 V vs. Li/Li^+ at the scan rate of 0.5 mV/s. After assembling of Swagelok cells, an Arbin 2000 instrument was used with the current densities of 0.04, 0.08 and 0.4 mA/cm^2, corresponding to the charge/discharge rate of C/10, C/5 and 1C, respectively.

3. Results and discussion

Several types of graphite and carbon black were used as conductive additives in the $LiCoO_2$ electrode. “SFG” and “SLC” are graphitic. Ketjenblack EC600 (hereafter referred to as Ket) and Super C65 (hereafter referred to as C65) are carbon black. The characteristics of all carbon sources that we examined are summarized in Table 1.

Table 1
The physicochemical properties of studied carbonaceous materials.

Name	Carbon type	SSA (m^2 g^{-1})[a]	Morphology	Density (g cm^{-3})[a]
SLC	Graphite	0.95	Spheroidized	–
SFG6L		16	Platelet	2.26
Ketjenblack 600	Carbon black	1400	Porous sphere	1.9
Super C65		62	Sphere	2.25

[a] The data are provided by the suppliers and are in good agreement with our measurements.

The morphologies of all provided carbon materials were investigated using TEM. The graphitic carbon (SFG) has a platelet-like shape, as shown in Fig. 1(a), and a specific surface area (SSA) of 16 m^2 g^{-1}. The SLC graphite has a spherical shape, as shown Fig. 1(b), with the lowest SSA of 0.95 m^2 g^{-1} among all of the examined carbon sources. The two carbon black sources both have spherical particles, as shown in Fig. 1(c) and (d), but they have different SSA values; Ket has a surface area that is more than 20 times greater (1400 m^2 g^{-1}) than that of C65 (SSA of 62 m^2 g^{-1}) due to its porous morphology, which is shown in the inset of Fig. 1(c). Graphitic materials generally have a lower SSA than carbon black materials.

Therefore, the significant differences between the two types of graphite and the two types of carbon black are the single particle shapes and the specific surface areas.

Based on these original characteristics of carbon, we prepared C–$LiCoO_2$ composites via ball-milling. The composite is mixed with a binder and solvent, and then the resulting paste is deposited on an aluminum current collector to create an electrode. A potentiostat was used to perform cyclic voltammetry measurements on these electrodes. The inset in Fig. 2 presents the cyclic voltammograms of the four different composite electrodes, SFG-, SLC-, C65- and Ket-$LiCoO_2$. The platelet-shaped graphite (SFG)-$LiCoO_2$ electrode exhibited well-defined redox peaks and the highest current densities for both the anodic and cathodic peaks among all of the composite electrodes. The anodic peak of the SLC graphite-$LiCoO_2$ electrode was significantly broader than the anodic peak of the platelet-shaped graphite (SFG)-$LiCoO_2$ electrodes. The super C65 carbon black-$LiCoO_2$ electrode presented clear redox peaks, whereas only half of an anodic peak and a broad cathodic peak were visible with the Ket electrode. In addition, the current densities of the anodic/cathodic peaks were the lowest for the Ket-$LiCoO_2$ electrode among all of the composite electrodes. In Fig. 2, the difference between anodic and cathodic peak positions is smallest for the SFG-$LiCoO_2$ electrode, as marked with the arrow, whereas the Ket-$LiCoO_2$ electrode has the largest difference between the anodic/cathodic peaks. It indicates that the cell with the SFG-$LiCoO_2$ electrode has a lower resistance than Ket-$LiCoO_2$ and the other composite electrodes. The widths of each anodic and cathodic peak are narrow for the SFG-$LiCoO_2$ electrode, while the width of the cathodic peak is the broadest for the Ket-$LiCoO_2$ electrode. The high current density and the short distance between the redox peaks in the cyclic voltammogram of the SFG-$LiCoO_2$ electrode indicate that this electrode has a lower resistance than the other electrodes.

We further investigated these cathodes by measuring their specific capacities at various charging rates after assembling the cathodes with a lithium metal anode and an electrolyte in a Swagelok cell. Fig. 3 shows the specific capacities of the C–$LiCoO_2$

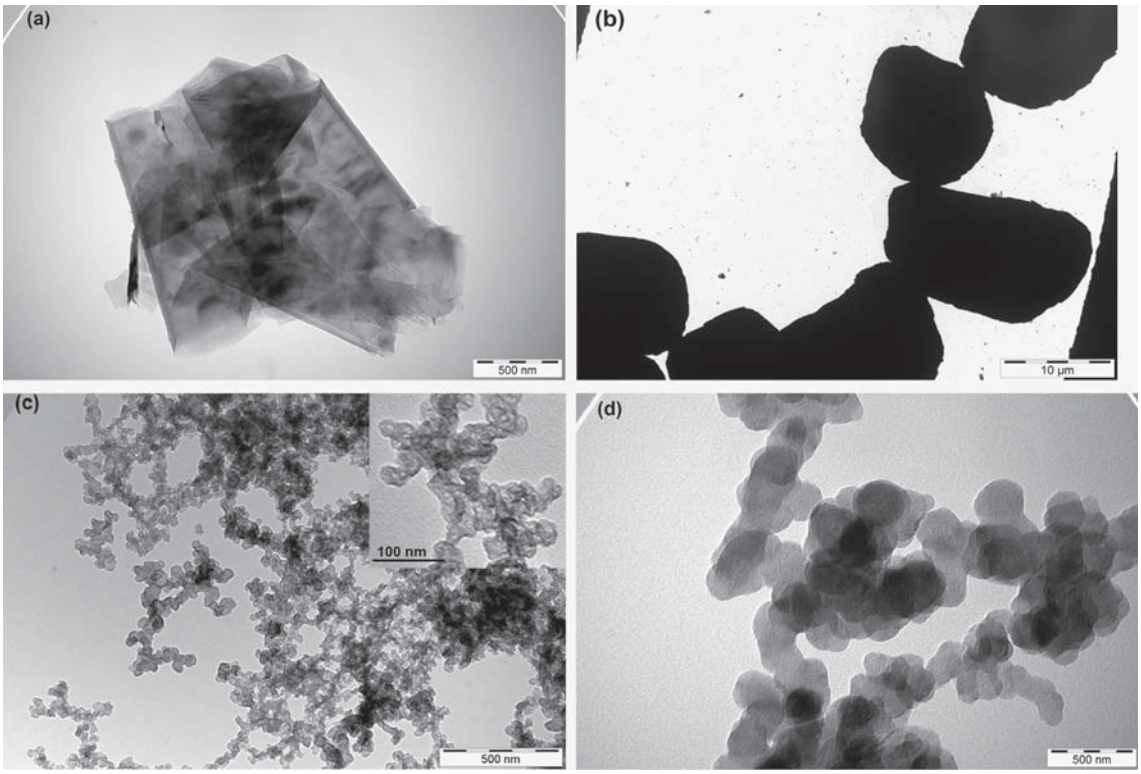

Fig. 1. TEM images of graphite and carbon black: (a) SFG platelet-like graphite, (b) SLC spherical graphite, (c) highly porous spherical Ket carbon black and (d) C65 spherical carbon black.

composites at charging rates of C/10 (charging in 10 h), C/5 (charging in 5 h) and 1C (charging in 1 h). The cell was tested for 5 cycles at each charging rate. The $LiCoO_2$ cathodes with graphitic SFG exhibited the highest capacities for all of the charging rates while the Ket carbon black presented the smallest capacity. This result is in good agreement with the cyclic voltammograms presented in Fig. 2. The amount of carbon is fixed to 20 wt% of $LiCoO_2$ in all composite electrodes. However, their capacities are different from each other as shown in Fig. 3. An electrochemically active cathode material should be conductive electronically and ionically in order to produce electrical energy during lithium insertion and extraction in lithium ion battery. Therefore, carbon is added in $LiCoO_2$ material to improve the electronic conductivity of cathode. A homogeneous structure of carbon and $LiCoO_2$ provides that electrons easily transfer to the current collector, resulting in high capacities of lithium ion batteries. On the other hand, an inhomogeneous structure of composite makes it difficult for electrons to travel through the cathode to the current collector due to the high

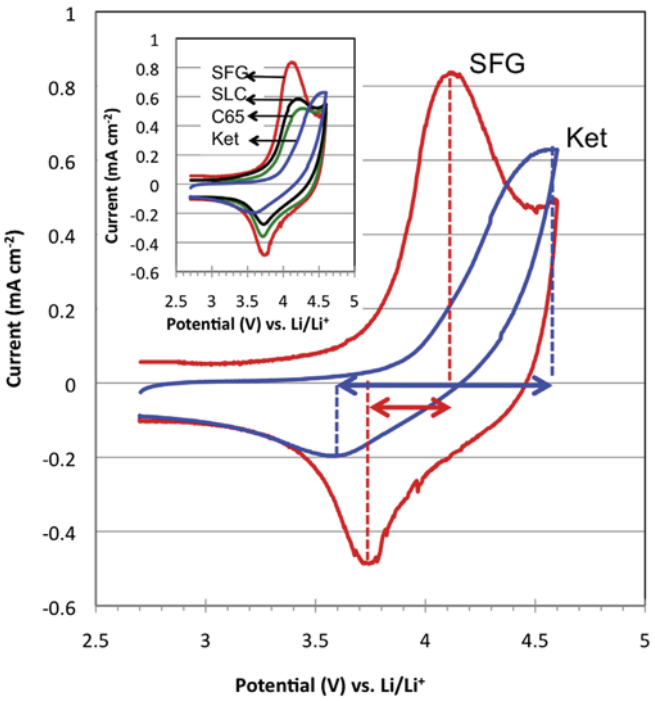

Fig. 2. Cyclic voltammograms of SFG- and Ket-$LiCoO_2$ composite cathodes. The inset figure shows the cyclic voltammograms of 4 different $LiCoO_2$ composite electrodes containing SFG, SLC, C65 or Ket carbon additive. The anode is Li metal and the electrolyte is EC:DMC with 1 M $LiPF_6$. The scan rate is 0.5 mV/s.

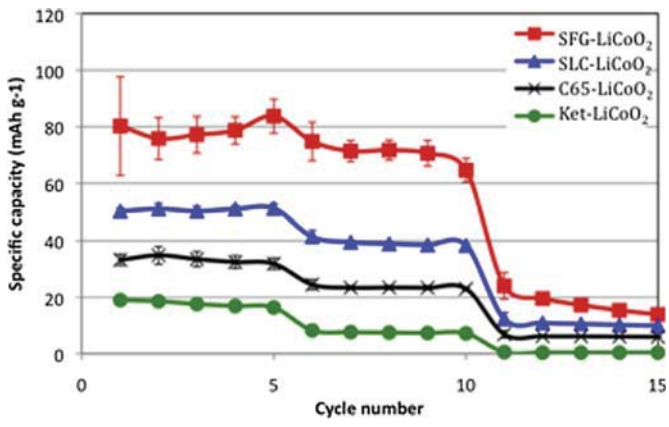

Fig. 3. The specific capacities at charging rate of C/10, C/5 and 1C with various types of carbon. Five cycles are measured at each charging rate. Three cells of each composite electrode are tested and their average deviation of each point is marked in the bar.

Table 2
The specific surface area of initial carbon and the composite of C–$LiCoO_2$ after ball-milling.

Cathode material	Carbon		Initial SSA of carbon ($m^2\ g^{-1}$)	SSA ($m^2\ g^{-1}$) of the composite	Morphology of the composite
$LiCoO_2$ (0.5 $m^2\ g^{-1}$)	SFG	Graphite	16	35.82	Rough surface, less agglomerations
	SLC	Spheroidized graphite	0.95	26.94	
	C65	Carbon black	62	22.58	Smooth surface, agglomeration, dense particles
	Ket600		1400	22.27	

resistance of the cathode. In the end, it leads to lower capacities of lithium ion batteries.

Surprisingly, the highly porous, 30-nm-sized Ket carbon black exhibited an inferior capacity compared to the other carbonaceous materials in the $LiCoO_2$ electrodes. In contrast, the same Ket carbon black exhibited a good electrochemical property with the nano-$LiMnPO_4$ composite, as shown in our previous report [22]. Therefore, the properties of the C–$LiCoO_2$ composite materials were studied.

The composites prepared with different carbonaceous materials via ball-milling exhibited different SSA values, as shown in Table 2. After ball-milling, the SFG-$LiCoO_2$ composite exhibited the highest SSA value of 36 $m^2\ g^{-1}$, whereas the initial SSA value of the SFG composite was the lowest. The spherical shaped graphite-$LiCoO_2$ composite has a medium SSA value of 26 $m^2\ g^{-1}$. However, the composites that contained carbon blacks (C65 and Ket) have the lowest SSA of 22–23 $m^2\ g^{-1}$ among all of the carbon–$LiCoO_2$ composites although those carbon blacks had the high SSA value (C65 : 62 $m^2\ g^{-1}$ and Ket : 1400 $m^2\ g^{-1}$) before ball-milling. The surface area of the composite is important for the use of liquid electrolytes because it represents the contact area between the cathode material and electrolyte. A composite cathode material with a larger specific surface area provides a larger contact area for the electrolyte, which consequently provides greater access for the lithium ions.

To understand these results, we investigated the effects of ball-milling on the micron- and nanosized particles separately. When the $LiCoO_2$ material was ball-milled for 60 min without the addition

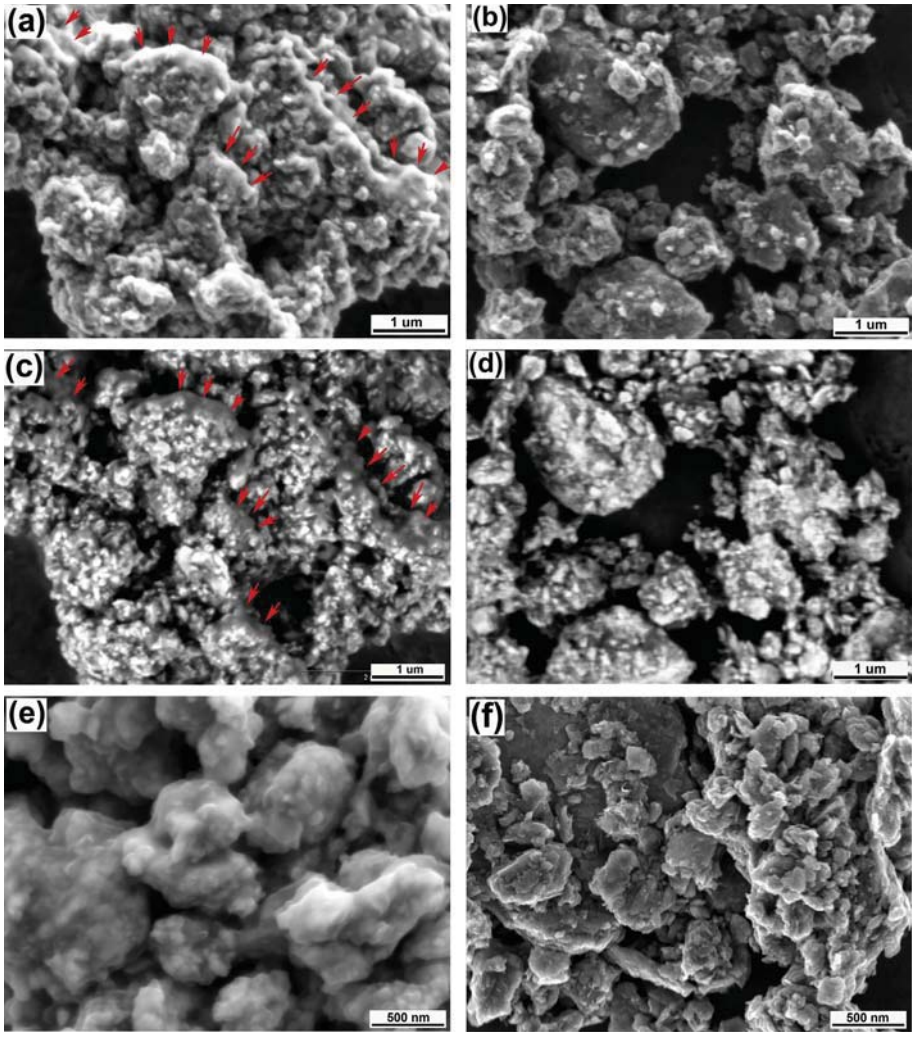

Fig. 4. SEM images of the composites, SFG graphite-$LiCoO_2$ (a, c and e) and Ket carbon black-$LiCoO_2$ (b, d and f). The images of (c) and (d) are backscattered electron images of SEM.

of carbon, the SSA of $LiCoO_2$ increased to 5 $m^2\ g^{-1}$ from the initial value of 0.5 $m^2\ g^{-1}$. This result indicates that the ball-milling process reduces the micron size of the $LiCoO_2$ particles. The SSA of the SFG-$LiCoO_2$ composite is greater than that of $LiCoO_2$ without SFG after ball-milling and the initial composite with SFG. This result indicates that the micron-sized graphite particles are also reduced via the ball-milling process. However, the C65 and Ket carbon black composites have SSAs values that are considerably less than the initial value. Therefore, both of the nanosized carbon black particles are formed through agglomeration, which results in a considerably lower surface area after ball-milling.

The morphologies of two composites, Ket-$LiCoO_2$ and SFG-$LiCoO_2$ after ball-milling were observed by two different modes, secondary and backscattered electron in SEM, as shown in Fig. 4. In the secondary electron image of Ket-$LiCoO_2$ composite, it exhibited a thick and smooth surface of agglomerates, which are indicated with arrows in Fig. 4(a). In order to clarify the identity of this thick layer, the backscattered electron mode in SEM was used because it can differentiate heavy (Co in $LiCoO_2$) and light (carbon) elements. Backscattered electron images collected during the SEM measurements confirmed that this thick surface appeared as a light color (gray), which indicates that it is a light element of carbon, and the other small particles appeared in a much brighter color (white), which indicates the presence of heavier elements of $LiCoO_2$, as shown in Fig. 4(c). However, the images of the SFG-$LiCoO_2$ composite presented in the secondary electron beam image of Fig. 4(b) and the backscattered electron image of Fig. 4(d) do not exhibit a significantly thick layer on the surface. Therefore, the SFG graphite forms as a thin coating layer on the $LiCoO_2$ particles. When the Ket-$LiCoO_2$ and SFG-$LiCoO_2$ composites are observed at a higher magnification, as shown in Fig. 4(e) and (f), respectively, we also observe a clear difference between these two composites. The surface of the Ket-$LiCoO_2$ composite appears smooth, whereas the surface of the SFG-$LiCoO_2$ composite exhibits sharp features. This smooth surface results from dense agglomeration of the Ket carbon black, which is coated on the $LiCoO_2$.

More detailed morphologies of the graphite and carbon black containing $LiCoO_2$ composites are revealed by the TEM images presented in Fig. 5. Fig. 5(a), (b) shows the TEM images of the composite SFG-$LiCoO_2$ after ball-milling. The shapes of the graphite and $LiCoO_2$ particles became polyhedral. Graphite (light gray in the images) covers the majority of the $LiCoO_2$ (black) surface as a thin layer (Fig. 5 (a)) and intimately contacts $LiCoO_2$ (Fig. 5(b)), whereas the Ket carbon black covers less of the $LiCoO_2$ surface due to the agglomeration of Ket, as shown in Fig. 5(c) and (d). This agglomeration of carbon black causes a thick layer on the $LiCoO_2$ particles, which is also shown in the SEM images of Fig. 4(a) and (c). Furthermore, the pores of the Ket carbon black particles disappear due to the dense agglomeration and ball-milling process.

Fig. 6 presents a schematic that illustrates how the composite structure evolves during ball-milling. Graphite has a layered, planer structure. In general, the layered sheets of graphite are stacked, as shown in the first left illustration of Fig. 6(a). These stacked layers of graphite can slide due to its lubricating property, and these layers can then separate to create a new surface, which consequently increases the surface area. The $LiCoO_2$ particles can easily attach to these large graphene planes of graphite during ball-milling (Fig. 6(a), middle). Furthermore, graphite acts as a lubricant and prevents the formation of large agglomerates during ball-milling. Consequently, the SFG-$LiCoO_2$ composite is a homogeneous

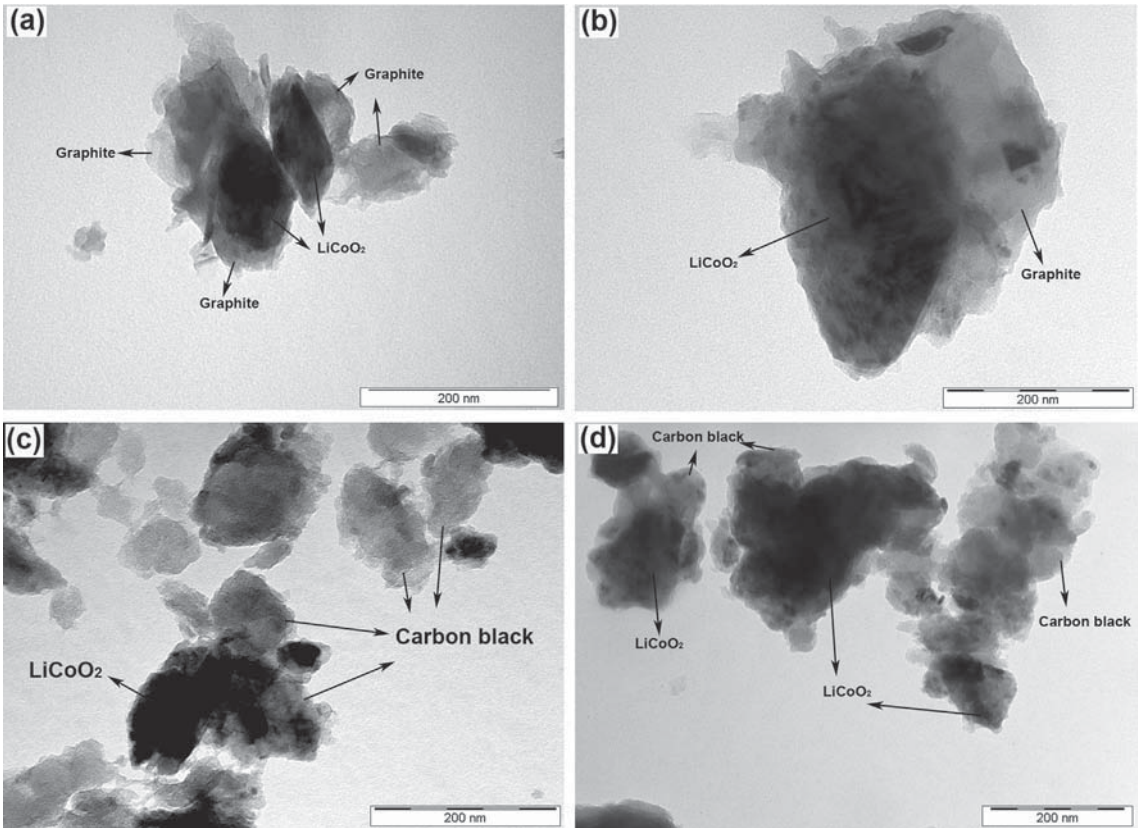

Fig. 5. TEM images of SFG-$LiCoO_2$ composite having a thin graphite layer, (a) and (b), and Ket-$LiCoO_2$ composite having large agglomerations of Ket carbon black, (c) and (d).

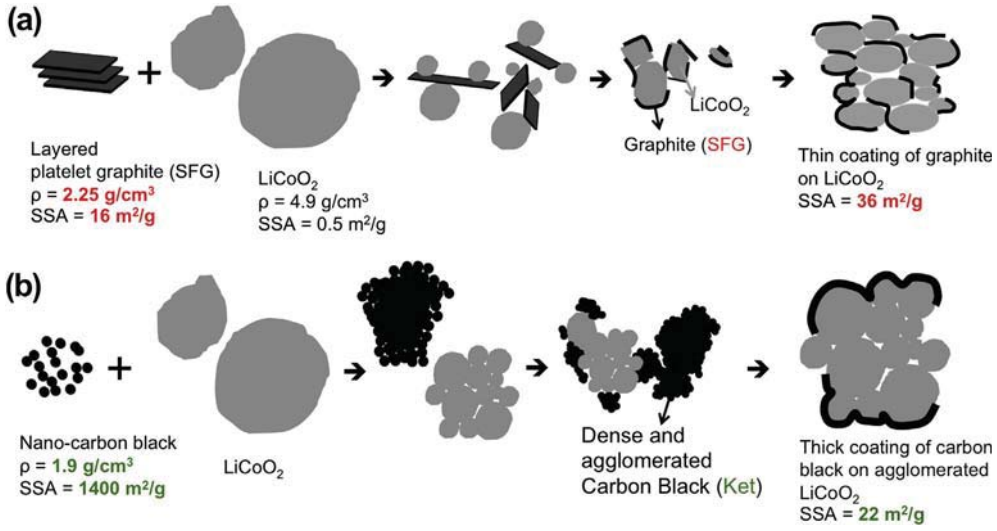

Fig. 6. Schematic illustration of ball-milling process with SFG platelet graphite, (a), and Ket carbon black, (b), containing $LiCoO_2$ composite.

mixture and has a large surface area with a thin layer of graphite that coats the surface of $LiCoO_2$ (Fig. 6(a) right). However, nano-Ket carbon black has one contact point because of its spherical shape rather than a 2D (plane) contact area such as graphite. Nanoparticles of Ket carbon black easily aggregate and separate from $LiCoO_2$ because of the physical characteristics of the nanoparticles and the lower powder density ($\rho = 1.9$ g cm^{-3}) compared to $LiCoO_2$ and graphite ($\rho = 2.25$ g cm^{-3}), which is illustrated in the middle of Fig. 6(b). Additionally, the pores of the nano-Ket particles are closed and become dense during the ball-milling process. This dense aggregation process forms a thick, solid coating layer on the $LiCoO_2$ particles, as illustrated in Fig. 6(b), right. Finally, the surface area of the Ket-$LiCoO_2$ composite decreases after the ball-milling process. This thick and dense coating consequently prevents the electrolyte from passing through the composite, which results in the poor electrochemical performance of the cathode.

However, our previous study revealed that the enhanced electrochemical performance of the nano-$LiMnPO_4$ cathode using nano-Ket carbon black in the composite was caused by the homogeneous composite structure of $LiMnPO_4$ and Ket carbon black [22]. The similar sizes of nanoparticles between carbon (20–30 nm) and $LiMnPO_4$ (15–30 nm in one dimension) can mix homogeneously, and the smaller difference of the powder densities (Ket is 1.9 g cm^{-3} and $LiMnPO_4$ is 3.45 g cm^{-3}) leads to less segregation during the ball-milling process. However, the nanosized carbon leads to agglomeration and distributes less homogeneously with the heavier ($\rho = 4.9$ g cm^{-3}) and micron-sized $LiCoO_2$ particles. In other words, the structure of the composite depends on not only the physicochemical characteristics of the carbon additive (i.e. particle size/shape and the lubricating property) but also on the characteristics of the active material (i.e. particle size and the density).

In summary, the physicochemical characteristics of the carbon additive affected the structure of the C–$LiCoO_2$ composite after ball-milling. We believe that the dependence of the different electrochemical properties of the $LiCoO_2$ electrode on the carbonaceous material is strongly related to the morphology of the $LiCoO_2$–carbon composite structure after ball-milling. For the graphite-$LiCoO_2$ composite, ball-milling provides a higher SSA by reducing the particle size of each component and by creating a homogeneous mixture with a thin carbon coating due to the lubricating property of graphite during ball-milling. This high SSA of the composite provides a larger contact area for the composite electrode and the electrolyte. The homogeneous mixture with a thin graphite carbon coating allows electrons and lithium ions to pass through the composite, which consequently results in superior capacities and better-determined cyclic voltammograms.

However, the initially nanosized carbon black agglomerated and separated from the heavy and micron-sized $LiCoO_2$ after the ball-milling process. This agglomeration and separation results in a low SSA of the composite and a thick carbon black layer on the $LiCoO_2$ materials. Finally, the electrochemical performance of the carbon black containing $LiCoO_2$ cathode is inferior to that of the graphite-containing cathode.

A thinner carbon-coating layer may be achieved by applying other methods, such as CVD or a thermal decomposition method in an inert atmosphere. However, the use of CVD is limited for upscaling, and thermal decomposition is limited for obtaining a pure and stoichiometric compound of $LiCoO_2$ due to the undesirable by-product in highly reductive environment.

The specific capacities in this report are relatively low compared to other reports [13,24–26]. These low capacities may result from a high resistance of the cell, such as interfacial resistance [27]. The reason of such a low electrochemical performance is not clear yet. However, the cyclic voltammograms clearly illustrate the different electrochemical behaviors of the graphite and carbon black-$LiCoO_2$ composite electrodes that were prepared by ball-milling. We are going to work on the origin of internal resistance in the cell using other characteristic analysis such as impedance. Furthermore, based on this work, we are currently investigating the optimized amount of carbon to maximize the energy density of the lithium ion batteries. We will also apply binary morphologies of carbon in the cathode materials using optimized ball-milling conditions that depend on the initial physicochemical properties of the carbonaceous materials.

4. Conclusions

We studied the effects of the carbonaceous materials used as conductive additives for $LiCoO_2$ cathode materials. The initial morphology and properties of the carbon additives affects the structure of the $LiCoO_2$–carbon composites via the ball-milling process and ultimately influences the electrochemical properties of the $LiCoO_2$ composite cathode. Platelet-shaped graphite provides well-defined redox peaks with anodic and cathodic peaks that are both narrow. However, spherical graphite (SLC) and high surface

area carbon black (Ket) provided broad redox peaks and a large separation between the anodic and cathodic peaks. We believe that the lubricating characteristics of the platelet graphite creates new surface area and provides more contact with the $LiCoO_2$ particles during the ball-milling process, whereas the spherical nanosized carbon black self-agglomerates. Finally, the $LiCoO_2$–graphite composite has a thin graphite coating layer and a more homogeneous mixture than the $LiCoO_2$–carbon black composite with a thick carbon layer.

Acknowledgments

This study was supported by the EKZ (Elektrizitätswerke des Kantons Zürich), the Swiss National Science Foundation (National Research Program 64), the FriMat (the Fribourg Center for Nanomaterials) and the University of Fribourg. The author thanks the Superior Graphite (USA Chicago), Timcal, (Belgium), Akzo Nobel (Germany) and Celgard (France) for providing carbon and the separator. The author is also grateful to Prof. Dr. Katharina M. Fromm for fruitful discussions and Christoph Neururer for the technical advice of SEM.

References

[1] K. Mizushima, P.C. Jones, P.J. Wiseman, J.B. Goodenough, Mater. Res. Bull. 15 (1980) 783–789.
[2] J.N. Reimers, J.R. Dahn, J. Electrochem. Soc. 139 (1992) 2091–2097.
[3] J. Cho, Y.J. Kim, B. Park, Chem. Mater. 12 (2000) 3788–3791.
[4] G.G. Amatucci, J.M. Tarascon, L.C. Klein, Solid State Ionics 83 (1996) 167.
[5] L. Lui, Z. Wang, H. Li, L. Chen, X. Huang, Solid State Ionics 152–153 (2002) 341–346.
[6] Y.J. Kim, J. Cho, T.J. Kim, B. Park, J. Electrochem. Soc. 150 (2003) A1723–A1725.
[7] T. Fang, J. Duh, S. Sheen, J. Electrochem. Soc. 152 (2005) A1701–A1706.
[8] L. Kavan, R. Bacsa, M. Tunckol, P. Serp, S.M. Zakeeruddin, F.L. Formal, M. Zukalova, M. Graetzel, J. Power Sources 195 (2010) 5360–5369.
[9] Q. Cao, H.P. Zhang, G.J. Wang, Q. Xia, Y.P. Wu, H.Q. Wu, Electrochem. Commun. 9 (2007) 1228–1232.
[10] H. Zheng, R. Yang, G. Liu, X. Song, V.S. Battaglia, J. Phys. Chem. C 116 (2012) 4875–4882.
[11] B.L. Cushing, J.B. Goodenough, Solid State Sci. 4 (2002) 1487–1493.
[12] R. Dominko, M. Gaberscek, J. Drofenik, M. Bele, J. Jamnik, Electrochim. Acta 48 (2003) 3709–3716.
[13] J.K. Hong, J.H.a . Lee, S.M. Oh, J. Power Sources 111 (2002) 90–96.
[14] C. Cai, Y. Wang, Materials 2 (2009) 1205–1238.
[15] H. Li, H. Zhou, Chem. Commun. 48 (2012) 1201–1217.
[16] X.M. Liu, Z.d. Huang, S.W. Oh, B. Zhang, P.C. Ma, M.M.F. Yuen, J.K. Kim, Compos. Sci. Technol. 72 (2012) 121–144.
[17] S. Luo, K. Wang, J. Wang, K. Jiang, Q. Li, S. Fan, Adv. Mater. 24 (2012) 2294–2298.
[18] M.M. Doeff, J.D. Wilcox, R. Kostecki, G. Lau, J. Power Sources 163 (2006) 180–184.
[19] J. Kim, B. Kim, J.-G. Lee, J. Cho, B. Park, J. Power Sources 139 (2005) 289–294.
[20] H. Takahara, T. Takeuchi, M. Tabuchi, H. Kageyama, Y. Kobayashi, Y. Kurisu, S. Kondo, R. Kanno, J. Electrochem. Soc. 151 (2004) A1539–A1544.
[21] M.M. Doeff, J.D. Wilcox, R. Yu, A. Aumentado, M. Marcinek, R. Kostecki, J. Solid State Electrochem 12 (2008) 995–1001.
[22] N.-H. Kwon, K.M. Fromm, Electrochim. Acta 69 (2012) 38–44.
[23] N.-H. Kwon, T. Drezen, I. Exnar, I. Teerlinck, M. Isono, M. Graetzel, Electrochem. Solid State Lett. 9 (2006) A277–A280.
[24] D.I. Choi, G.-B. Han, D.J. Lee, J.-K. Park, J.W. Choi, J. Electrochem. Soc. 158 (2011) A1150–A1154.
[25] M. Jo, Y.-S. Hong, J. Choo, J. Cho, J. Electrochem. Soc. 156 (2009) A430–A434.
[26] X. Li, F. Cheng, B. Guo, J. Chen, J. Phys. Chem. B 109 (2005) 14017–14024.
[27] H.-C. Wu, E. Lee, N.-L. Wu, T.R. Jow, J. Power Sources 197 (2012) 301–304.